Peak in the static structure factor of a Bose-Einstein condensate

J. Steinhauer,[1] R. Ozeri,[2,3] N. Katz,[2] and N. Davidson[2]
[1]*Department of Physics, Technion—Israel Institute of Technology, Technion City, Haifa 32000, Israel*
[2]*Department of Physics of Complex Systems, Weizmann Institute of Science, Rehovot 76100, Israel*
[3]*Time and Frequency Division, National Institute of Standards and Technology, Boulder, Colorado 80305, USA*
(Received 22 June 2004; revised manuscript received 15 April 2005; published 15 August 2005)

A peak in the static structure factor of a Bose-Einstein condensate is computed, both near and far from a Feshbach resonance. A low-density approximation is made, allowing for an analytic result. A Monte Carlo calculation shows that the peak is larger than predicted by the low-density approximation, for the upper range of densities considered here. The peak could be measured by a probe beam of cold atoms.

DOI: 10.1103/PhysRevA.72.023608 PACS number(s): 03.75.Kk, 61.20.−p, 67.40.Db

The static structure factor $S(k)$ of a Bose-Einstein condensed fluid can display a peak exceeding unity, the value for an uncorrelated gas. This peak occurs for excitations whose wavelength $2\pi/k$ is equal to the characteristic wavelength of density fluctuations in the ground-state wave function of the quantum fluid. Superfluid ^{4}He exhibits such a peak which, via the Feynman-Bijl relation [1], corresponds to the roton minimum in the excitation spectrum $\omega(k)$ [2].

Feynman [1] described several possible microscopic pictures of a roton in superfluid ^{4}He. He found that the most likely description is that the roton is analogous to a single atom moving through the condensate, with wave number k close to $2\pi/n^{-1/3}$, where $n^{-1/3}$ is the mean atomic spacing.

The peak in $S(k)$ in superfluid ^{4}He was calculated by a Monte Carlo technique [3,4] using a many-body Jastrow wave function [5], which is of the form

$$\psi = \prod_{j>i=1}^{N} f(|\mathbf{r}_i - \mathbf{r}_j|), \tag{1}$$

where the pair function $f(r)$ should be determined for the quantum fluid under consideration. The wave function (1) deviates significantly from unity if any two atoms become very close to one another. For superfluid ^{4}He, the two-particle correlation function $g(r)$ for this wave function has fluctuations with a preferential length scale of $n^{-1/3}$, which results in a peak greater than unity in $S(k)$ near $k \approx 2\pi/n^{-1/3}$, in agreement with Feynman's picture.

Both Feynman's result and the results of the Jastrow wave function roughly agree with measurements [6] of $S(k)$ and $\omega(k)$.

The Jastrow wave function (1) has also been considered for a low-density Bose-Einstein condensate (BEC) [3], and has been used to compute various properties of a high-density BEC [7]. In both of these works, $f(r)$ is taken as the solution of the two-body Schrödinger equation. We employ such a Jastrow wave function to compute the peak in $S(k)$ for a low-density BEC.

By an analytic calculation, we find that the diameter r_0 of the atoms determines the location of the peak in $S(k)$, rather than $n^{-1/3}$. We see that Feynman's view that $n^{-1/3}$ is the relevant length scale is the special case of high density, for which $r_0 \approx n^{-1/3}$.

In a low-density BEC, Feynman's view of the roton as a single atom moving through the condensate seems natural. In general, the excitation spectrum of a low-density BEC is of the Bogoliubov form [9,10], which consists of phonons and single-particle excitations. We find that the peak in $S(k)$ occurs on the single-particle part of the spectrum, at $k \approx 8/\pi a$, where a is the s-wave scattering length.

Although the general form of the wave function (1) can be applied to both superfluid ^{4}He and BEC, the wave function is fundamentally different for these two quantum fluids. For both of these fluids, below some temperature $T_{s\text{-wave}}$, the thermal de Broglie wavelength λ_{dB} becomes longer than the characteristic length scale R of the interparticle potential. Below $T_{s\text{-wave}}$, all scattering processes except for s-wave scattering become negligible. Since a BEC is a dilute gas, $n^{-1/3}$, which is typically about 1500 Å, is much larger than R. Therefore, the critical temperature T_c for quantum degeneracy, at which λ_{dB} becomes comparable to $n^{-1/3}$, is much lower than $T_{s\text{-wave}}$. Therefore, only s-wave scattering plays a role here for a BEC. In contrast to BECs, superfluid ^{4}He is a relatively dense liquid, for which $n^{-1/3}$ is comparable to R. Therefore, the temperature $T_{s\text{-wave}}$ also marks the transition T_c to quantum degeneracy. Even below T_c for superfluid ^{4}He, partial waves other than the s wave contribute to the wave function.

For many properties of a BEC, a is sufficient to describe the interparticle potential, and the form of the potential does not play a role [11,12]. To quantitatively describe the peak in $S(k)$, however, the s-wave scattering wave function must be known to interparticle separations somewhat smaller than R, where the details of the potential are relevant.

Rotons have been predicted in a BEC in the presence of optical fields [13–15], as well as in a dipolar BEC [16]. In this work, we find that a peak in $S(k)$ occurs in an unperturbed BEC without any dipole interaction. We consider the enhancement of this peak near a Feshbach resonance [17,18], but the physics is qualitatively the same as in the unperturbed case.

We use a low-density approximation [5] to compute $g(r)$ and the peak in $S(k)$ for a BEC with a positive scattering length. The low-density approximation is compared to a Monte Carlo calculation.

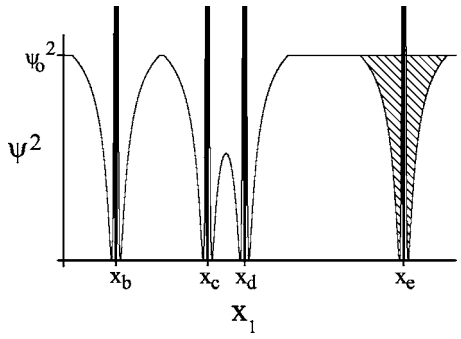

FIG. 1. Schematic one-dimensional representation of the Jastrow wave function. The dependence on the single dimension x_1 is shown. The overall scaling of the curve is given by the factors in the wave function not involving x_1. The labeled values of x_1 correspond to the positions of atoms other than atom 1. x_1 varies over one dimension of the volume V.

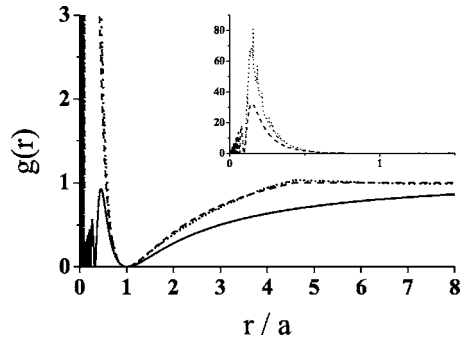

FIG. 2. The two-particle correlation function for a BEC. The solid and dashed curves are the low-density approximation (4) with (2), with $na^3=2.2\times10^{-4}$ and 0.011, respectively. The dotted curve is the Monte Carlo result for $na^3=0.011$. For $na^3=2.2\times10^{-4}$, the Monte Carlo result is indistinguishable from the solid curve. The inset shows the curves for $na^3=0.011$ only.

For a BEC of alkali-metal atoms, the potential can be taken as the van der Waals potential $-C_6/r^6$ for atomic separations r greater than a few angstroms [19,20]. For this potential, R is given by $(mC_6/\hbar^2)^{1/4}$, which ranges from about 50 to 100 Å [20,21]. The wave function for s-wave scattering between two particles in the limit of zero energy is given by $\psi_6(r)$, which is the solution of the radial Schrödinger equation with the van der Waals potential. $\psi_6(r)$ can be written in terms of elliptic integrals [19]. For $r>R$, this wave function is very close in form to $1-a/r$ [11,22]. For the case of $a \gg R$, $\psi_6(r)$ therefore obtains large negative values for $r \ll a$ [23]. It is important to note that this behavior is very different from the wave function of the hard-sphere gas, which is zero for $r<a$ [11]. As we will see, these large negative values for $r \ll a$ greatly increase the height of the peak in $S(k)$ for the BEC relative to the hard-sphere gas, in the limit of $a \gg R$.

We do not use $\psi_6(r)$ as $f(r)$ in Eq. (1), because even for $r \gg n^{-1/3}$, $\psi_6(r)$ is significantly less than unity. This is nonphysical, in the sense that no matter how large the volume of the gas for fixed density, the value of the many-body wave function (1) depends on the volume. To account for many-body effects, we use the following pair function which goes to unity for $r>n^{-1/3}$ [7,20]:

$$f(r) = \begin{cases} \psi_6(r)/\psi_6(n^{-1/3}) & (r \leqslant n^{-1/3}), \\ 1 \quad (r > n^{-1/3}). \end{cases} \tag{2}$$

While using Eq. (2) rather than $\psi_6(r)$ as $f(r)$ is more physically correct, we have verified that both functions give essentially the same result for the peak in $S(k)$.

To compute (2), R is needed. Throughout this work, we use $R=0.05n^{-1/3}$. This is a typical experimental value, and the results here are rather insensitive to R.

Equation (1) with (2) is shown schematically in Fig. 1. To aid in visualization, Fig. 1 shows the wave function squared in one dimension, as a function of the position x_1 of atom number 1. The positions of all of the other atoms, such as atoms b through e, are fixed. As long as atom number 1 is far from the other atoms, the wave function has the constant value ψ_0. This value is determined by the positions of the atoms other than x_1. The rapid oscillations in $\psi_6(r)$ for $r<R$ appear in Fig. 1 as dark vertical bands, when atom number 1 is very close to another atom.

The correlation function $g(r)$ gives the unconditional probability of two atoms being at a distance r. $g(r)$ is related to the pair function $f(r)$ by [5]

$$g(|\mathbf{r}_1-\mathbf{r}_2|) = V^2 \frac{\int d\mathbf{r}_3 \cdots d\mathbf{r}_N \prod_{j>i=1}^{N} f^2(|\mathbf{r}_i-\mathbf{r}_j|)}{\int d\mathbf{r}_1 \cdots d\mathbf{r}_N \prod_{j>i=1}^{N} f^2(|\mathbf{r}_i-\mathbf{r}_j|)}, \tag{3}$$

where the integrals are over the volume V. Equation (3) can be evaluated starting with the first integral in the denominator, $\int d\mathbf{r}_1 \Pi_{j>1}^{N} f^2(|\mathbf{r}_1-\mathbf{r}_j|)$. This can be visualized as the integral over the function shown in Fig. 1 for one dimension. Neglecting three-body interactions greatly simplifies this integral. Three-body interactions are rare for small values of the gas parameter na^3, assuming that the range of three-body interactions is of the same order of magnitude as the range of two-body interactions. A three-body interaction is represented in Fig. 1 by the points x_c and x_d, where atoms 1, c, and d interact. Neglecting such interactions, the integral is a function of the volume v indicated by the shaded region in Fig. 1. The integral is then given by $V-(N-1)v$, where $v = V-\int d\mathbf{r}\, f^2(r)$. This result is independent of the positions of the $\mathbf{r}_j$.

Evaluating all of the integrals in (3) similarly to the first yields $g(|\mathbf{r}_1-\mathbf{r}_2|) \approx V^2 f^2(|\mathbf{r}_1-\mathbf{r}_2|)[(V-v)V]^{-1}$. Since $V \gg v$, we obtain the result of the low-density approximation [5]

$$g(r) \approx f^2(r). \tag{4}$$

The result (4) with (2) is indicated by the solid curve in Fig. 2 for $na^3=2.2\times10^{-4}$. This value of na^3 is an order of magnitude greater than typical experimental values without a Feshbach resonance. The result for $na^3=0.011$ is also shown in the figure.

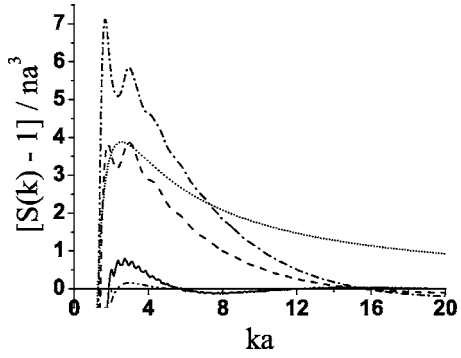

FIG. 3. The peak in $S(k)$ for a BEC, computed by Eq. (5). The dash-dotted and solid curves are the Monte Carlo results for $na^3=0.011$ and 2.2×10^{-4}, respectively. The result of the low-density approximation (4) with (2) for $na^3=0.011$ is indicated by the dashed curve. The result of the low-density approximation for $na^3=2.2\times10^{-4}$ is indistinguishable from the solid curve. The dotted curve is the small-R limit, given by Eq. (6). The dash-double-dotted curve indicates the hard-sphere gas in the limit of low density, given by Eq. (7).

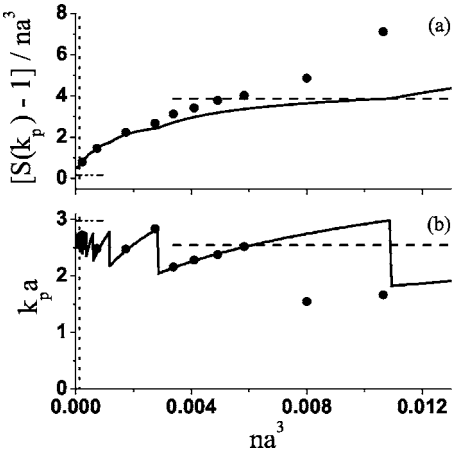

FIG. 4. The height (a) and location (b) of the peak in $S(k)$ for a BEC, as a function of na^3. The circles are the Monte Carlo result. The solid curves are the low-density approximation. The dashed curves are the analytic small-R limit. The dash-double-dotted curves indicate the hard-sphere gas in the limit of low density. The dotted lines indicate nR^3.

While (4) is useful for obtaining analytic results, a more accurate computation can be made by the Monte Carlo technique described in Ref. [3]. This technique effectively evaluates (3) by using a Metropolis algorithm to randomly choose configurations of the N atoms ($N=100$ here), according to the probability distribution given by (1) with (2), and computing the distribution of distances between the atoms, with periodic boundary conditions. This distribution, averaged over many likely configurations, is proportional to $r^2g(r)$. The result of the Monte Carlo computation is shown in Fig. 2 for $na^3=2.2\times10^{-4}$ and 0.011. These results were obtained with 9×10^8 and 2×10^7 iterations, respectively.

The small oscillations for small r shown in Fig. 2 are negligible in the computation of the static structure factor. These are the oscillations for r values less than that of the first large peak below $r/a=1$, in the solid and dashed curves. To save computing time these oscillations are not included in $f^2(r)$ in the Monte Carlo computation.

For a sufficiently wide and tall peak below $r/a=1$, a cluster of atoms can be stable. For the largest values of na^3 considered here, such clusters can suddenly form, long after the Monte Carlo computation has reached equilibrium. We detect and avoid these clusters by observing the drastic increase in $g(r<a)$, as was done in [24], and discussed in [3], for a gas-solid phase transition.

The static structure factor $S(k)$ is given by $1+n\int[g(r)-1]e^{i\mathbf{k}\cdot\mathbf{r}}d\mathbf{r}$, which in general can be written [25]

$$S(k) = 1 + 4\pi n \int_0^\infty dr\, r^2[g(r)-1]\frac{\sin(kr)}{kr}. \tag{5}$$

We use Eq. (5) to compute $S(k)$ for the low-density approximation (4) with (2), as indicated in Fig. 3. The height $S(k_p)$ and location k_p of the peak in $S(k)$ are indicated by the solid curves of Fig. 4. $S(k)$ in Fig. 3 has several maxima, the tallest of which is taken as the relevant maximum. As na^3 is varied, the peak which is the tallest varies, resulting in the jagged appearance of the solid curves of Fig. 4.

For the Monte Carlo computation, $S(k)$ is found by inserting $g(r)$ such as is shown in Fig. 2 into Eq. (5). The results are indicated in Fig. 3 by the dash-dotted and solid curves. For small na^3, the height and location of the peak in $S(k)$ are seen in Fig. 4 to be the same for the low-density approximation and the Monte Carlo result. The low-density approximation is therefore valid for small na^3. For the larger values of na^3, the height of the peak in the Monte Carlo calculation is larger than that of the low-density approximation, as seen in Fig. 4(a).

By applying the low-density approximation to the limit of $a\gg R$, we can obtain an analytic expression for $S(k)$ for $R\ll a\ll n^{-1/3}$. In this range, $f(r)$ can be taken as $1-a/r$ for all r, including values well below $r=a$, as indicated by the dotted curve of Fig. 5. By Eqs. (4) and (5),

$$S(k) = 1 + 4\pi na^3[\pi(ka)^{-1}/2 - 2(ka)^{-2}]. \tag{6}$$

This small-R limit is indicated by the dotted curve in Fig. 3. The height of the peak in $S(k)$ in this limit is $S(k_p)=1$

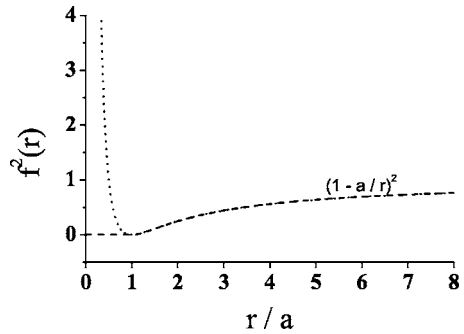

FIG. 5. The pair function in the small-R limit (dotted curve). The pair function for the hard-sphere gas in the limit of low density is shown for comparison (dashed curve).

$+\pi^3 na^3/8$, and the location is given by $k_p = 8/\pi a$. These values are indicated by the dashed curves of Fig. 4, which as expected, agree with the low-density approximation (solid curves) for $a \gg R$, where nR^3 is indicated by the dotted lines. As seen in the above expression for k_p, the location of the peak in $S(k)$ is determined by a, rather than by $n^{-1/3}$.

$S(k)$ given by (6) is very different from the expression for the hard-sphere gas in the limit of low density, for which $f(r)$ can be taken as $1-a/r$ for $r>a$ but $f(r)$ is zero for $r<a$ [26,27], as indicated by the dashed curve in Fig. 5. The hard-sphere gas does not have the large peak in $f^2(r)$ for $r<a$ which is present in the small-R limit, as seen in the dotted curve of Fig. 5. By Eqs. (4) and (5) for the hard-sphere gas,

$$S(k) = 1 + 4\pi na^3 \left((ka)^{-3}[ka\cos(ka) - \sin(ka)] - 2(ka)^{-2}\cos(ka) + (ka)^{-1}\int_{ka}^{\infty} du \frac{\sin u}{u} \right). \quad (7)$$

This low-density limit for the hard-sphere gas is indicated by the dash-double-dotted curve in Fig. 3. The height of the peak for the hard-sphere gas is given by $S(k_p) = 1 + 0.15na^3$, and the location is given by $k_p = 3/a$, as shown in Fig. 4. It is thus seen that the peak in $S(k)$ in the small-R limit is an order of magnitude taller than for the hard-sphere gas in the limit of low density. This is due to the large peak in $g(r)$ for $r < a$ in the small-R limit. We see that the measurement of $S(k)$ is a sensitive technique for probing $g(r)$ for $r<a$.

The peak in $S(k)$ for the hard-sphere gas can also be found from the roton minimum in the excitation spectrum of the hard-sphere gas for low densities, computed in [28–30]. The results from these works vary, but in all cases the resulting peak in $S(k)$ is roughly an order of magnitude smaller than the peak in the small-R limit reported here.

For $na^3 = 0.011$, the height of the peak in $S(k)$ given by the Monte Carlo calculation is $S(k_p) = 1.08$, as shown in Figs. 3 and 4(a). Measuring this 8% effect could be experimentally feasible. $na^3 = 0.011$ could be attained by a Feshbach resonance [22]. It should be noted, though, that for this relatively large value of na^3, the form of (2) is only approximate, so the expressions for the height and location of the peak should be considered as estimates only.

Due to phonons, the true $S(k)$ is proportional to k for $k \lesssim \xi^{-1}$, where $\xi^{-1} = a^{-1}\sqrt{8\pi na^3}$ is the inverse healing length. The curves shown in Fig. 3 do not show this linear behavior for small k because the wave function (1) with (2) does not have the long-range correlations of a phonon [3,4].

For superfluid ^{4}He the three inverse length scales $2\pi/n^{-1/3}$, k_p, and ξ^{-1}, are roughly equal. This is also true for a relatively large value of a in a BEC. As na^3 increases, both k_p and ξ^{-1} approach $2\pi/n^{-1/3}$. More precisely, the ratios of ξ^{-1} and k_p to $2\pi/n^{-1/3}$ are $\sqrt{2/\pi}(na^3)^{1/6}$ and approximately $4/\pi^2(na^3)^{-1/3}$, respectively. The latter ratio implies that an appropriate measurement system for measuring a peak in $S(k)$ should be able to probe wavelengths somewhat shorter than $n^{-1/3}$.

A beam of cold atoms is a suitable probe for such a measurement. This beam would be analogous to a beam of neutrons used for measuring $S(k)$ for superfluid ^{4}He [8]. An atom laser, in which the atoms are accelerated by gravity, is one example of such a beam [31–33]. Another example is a cloud of cold atoms accelerated by a moving magnetic trap [34]. The beam should be of a different atomic species than the BEC, to avoid a Feshbach resonance between the probe and the BEC.

For the densities shown in Fig. 4, the momentum required for the beam is low enough that the interaction between the probe beam and the target BEC would be s-wave scattering only. The collision products would therefore fall on a sphere in momentum space, as observed by absorption imaging [34–36]. The probability of an atom scattering into a particular angle is proportional to $S(k)$, in analogy to neutron scattering experiments. The absorption image of the atoms would therefore show a preferred angle, corresponding to the peak in $S(k)$.

The required velocity of the probe atoms depends on their mass. For typical species used in cold atom experiments, such as rubidium or sodium, the probe atoms should have a velocity on the order of 100 mm sec^{-1} to probe the higher-density points in Fig. 4. Such velocities are readily obtainable [31–34].

In conclusion, we find the height $S(k_p)$ and location k_p of the peak in the BEC static structure factor, for a range of densities. A low-density approximation is compared to a Monte Carlo calculation. The values of $S(k_p)$ and k_p given by the two methods agree for the lowest densities. For higher densities, the Monte Carlo calculation predicts an enhancement in $S(k_p)$ of almost a factor of 2 over the low-density approximation.

In contrast to the Monte Carlo calculation for superfluid ^{4}He, the small-R limit gives explicit expressions for the height and location of the peak in $S(k)$.

We thank Servaas Kokkelmans, Ady Stern, Yoseph Imry, Daniel Kandel, Eric Akkermans, Johnny Vogels, and Ananth Chikkatur for helpful discussions. This work was supported by the Israel Science Foundation and the Israel Ministry of Science. J.S. acknowledges support by the Taub and Shalom Foundations.

[1] R. P. Feynman, Phys. Rev. **94**, 262 (1954).
[2] L. Landau, J. Phys. (USSR) **11**, 91 (1947).
[3] W. L. McMillan, Phys. Rev. **138**, 442 (1965).
[4] D. Schiff and L. Verlet, Phys. Rev. **160**, 208 (1967).
[5] R. Jastrow, Phys. Rev. **98**, 1479 (1955).
[6] D. G. Henshaw, Phys. Rev. **119**, 9 (1960). For additional references, see [3], [4], or [11].
[7] S. Cowell, H. Heiselberg, I. E. Mazets, J. Morales, V. R. Pan-

dharipande, and C. J. Pethick, Phys. Rev. Lett. **88**, 210403 (2002).
[8] Ph. Nozieres and D. Pines, *The Theory of Quantum Liquids* (Addison-Wesley, Reading, MA, 1990), Vol. II.
[9] N. N. Bogoliubov, J. Phys. (USSR) **11**, 23 (1947).
[10] J. Steinhauer, R. Ozeri, N. Katz, and N. Davidson, Phys. Rev. Lett. **88**, 120407 (2002).
[11] K. Huang, *Statistical Mechanics* (John Wiley & Sons, New York, 1987).
[12] F. Dalfovo, S. Giorgini, L. P. Pitaevskii, and S. Stringari, Rev. Mod. Phys. **71**, 463 (1999).
[13] J. Higbie and D. M. Stamper-Kurn, Phys. Rev. Lett. **88**, 090401 (2002).
[14] D. H. J. O'Dell, S. Giovanazzi, and G. Kurizki, Phys. Rev. Lett. **90**, 110402 (2003).
[15] Z. Nazario and D. I. Santiago, J. Low Temp. Phys. **137**, 599 (2004).
[16] L. Santos, G. V. Shlyapnikov, and M. Lewenstein, Phys. Rev. Lett. **90**, 250403 (2003).
[17] Herman Feshbach, Ann. Phys. (N.Y.) **5**, 357 (1958).
[18] S. Inouye, M. R. Andrews, J. Stenger, H.-J. Miesner, D. M. Stamper-Kurn, and W. Ketterle, Nature (London) **392**, 151 (1998).
[19] G. F. Gribakin and V. V. Flambaum, Phys. Rev. A **48**, 546 (1993).
[20] A. J. Leggett, Rev. Mod. Phys. **73**, 307 (2001).
[21] M. Marinescu, H. R. Sadeghpour, and A. Dalgarno, Phys. Rev. A **49**, 982 (1994).
[22] Using the formalism of S. J. J. M. F. Kokkelmans, J. N. Milstein, M. L. Chiofalo, R. Walser, and M. J. Holland, Phys. Rev. A **65**, 053617 (2002), we find that a is well-defined close to a Feshbach resonance, for the values of a considered here, and for the collisional energies found in the ground state of a BEC.
[23] J. Dalibard, in *Proceedings of the International School of Physics "Enrico Fermi," Course CXL* (IOS, Amsterdam, 1999).
[24] W. W. Wood and J. D. Jacobson, J. Chem. Phys. **27**, 1207 (1957).
[25] R. P. Feynman and M. Cohen, Phys. Rev. **102**, 1189 (1956).
[26] T. D. Lee, K. Huang, and C. N. Yang, Phys. Rev. **106**, 1135 (1957).
[27] A. Isihara and D. W. Jepsen, Phys. Rev. **158**, 112 (1967).
[28] K. A. Brueckner and K. Sawada, Phys. Rev. **106**, 1128 (1957).
[29] L. Liu, L. S. Liu, and K. W. Wong, Phys. Rev. **135**, A1166 (1964).
[30] W. E. Parry and D. ter Haar, Ann. Phys. (N.Y.) **19**, 496 (1962).
[31] I. Bloch, T. W. Hänsch, T. Esslinger, Phys. Rev. Lett. **82**, 3008 (1999).
[32] E. W. Hagley, L. Deng, M. Kozuma, J. Wen, K. Helmerson, S. L. Rolston, and W. D. Phillips, Science **283**, 1706 (1999).
[33] M.-O. Mewes, M. R. Andrews, D. M. Kurn, D. S. Durfee, C. G. Townsend, and W. Ketterle, Phys. Rev. Lett. **78**, 582 (1997).
[34] N. R. Thomas, N. Kjærgaard, P. S. Julienne, and A. C. Wilson, Phys. Rev. Lett. **93**, 173201 (2004).
[35] A. P. Chikkatur, A. Görlitz, D. M. Stamper-Kurn, S. Inouye, S. Gupta, and W. Ketterle, Phys. Rev. Lett. **85**, 483 (2000).
[36] N. Katz, J. Steinhauer, R. Ozeri, and N. Davidson, Phys. Rev. Lett. **89**, 220401 (2002).